

Original Research Article

Tunica intima compensation for reduced stiffness of the tunica media in aging renal arteries as measured with scanning acoustic microscopy

Short title: Aging of renal arteries measured by scanning acoustic microscope

Katsutoshi Miura*

<https://orcid.org/0000-0002-9262-7702>

Department of Health Science, Pathology and Anatomy, Hamamatsu University School of Medicine, Hamamatsu, Japan

*Corresponding author

E-mail: kmiura.hama.med@gmail.com (KM)

Abstract

Objectives

Aging causes stiffness and decreased function of the renal artery (RA). Histological study with light microscopy can reveal microscopic structural remodeling but no functional changes. The present study aimed to clarify the association between structural and functional aging of the RA through the use of scanning acoustic microscopy.

Methods

Formalin-fixed, paraffin-embedded cross-sections of renal arteries from 64 autopsy cases were examined. Speed-of-sound (SOS) values of three layers, which correspond to the stiffness, were compared among different age groups. SOS of the tunica media was examined in terms of blood pressure (BP) and SOS of the ascending aorta. Vulnerability to proteases was assessed by SOS reduction after collagenase treatment.

Results

The tunica intima presented inward hypertrophy with luminal narrowing, and the tunica media showed outward hypertrophic remodeling with aging. SOS of the tunica media and internal and external elastic laminae showed a reverse correlation with age. SOS of the tunica media was negatively correlated with BP and strongly associated with that of the aorta. The tunica media of young RAs were more sensitive to collagenase compared with

32 the old ones.

33 **Conclusions**

34 Scanning acoustic microscopy is useful for observing the aging process of the RA. This
 35 technique simultaneously shows structural and mechanical information from each portion
 36 of the RA. In the process of aging, the RA loses contractile function and elasticity as a
 37 result of protease digestion. The tunica media and the internal and external elastic laminae
 38 exhibit reduced stiffness, but the tunica intima stiffens with atherosclerosis. As a
 39 consequence, the RA's outer shape changes from round to oval with inward and outward
 40 hypertrophy. This indicates that the inner resistant intima supports the mechanical
 41 weakness of the tunica media to compensate for an increase in BP with aging.

42

Introduction

Arterial stiffness is the consequence of structural and functional changes of the vascular wall that occur in response to cardiorenal metabolic syndrome, injury, or aging.[1]

Measurements of functional change in renal arteries (RAs) include central pulse pressure/stroke volume index, pulse wave velocity (PWV), total arterial compliance, pulse pressure (PP), and augmentation index.[2] PWV and PP, in particular, are two significant indices of arterial stiffness[3] that typically increase with age.[4]

Conventional imaging methods involved in the diagnostic modalities of RAs are Doppler ultrasonography, scintigraphy, computed tomographic angiography, magnetic resonance arteriography, and angiography.[5][6] However, only histological study with light microscopy (LM) can reveal microscopic structural changes. LM information contributes to the detection of morphological alteration but not functional changes such as tissue stiffness or fragility. Although aging RAs usually show severe atherosclerosis and calcification, the aging process of other layers, such as tunica media, is not well known. Smooth muscles may lose contractile function and corresponding structural changes may occur with aging.

The aging process is commonly associated with increased vascular rigidity and decreased vascular compliance.[5] Although several researchers have reported functional

or structural changes associated with aging,[1]·[7] simultaneous acquisition of structural and functional information with the same histological specimen is rare. If histological and functional information can be obtained simultaneously from the same slide, the association of mechanical and the corresponding structural changes in the aging process may be more understandable and precise for comparing lesions.

Scanning acoustic microscopy (SAM) reveals morphological information and mechanical properties because speed-of-sound (SOS) through tissues corresponds to the stiffness of the content.[8]·[9]·[10]·[11] Simultaneous detection of histological structure and the corresponding tissue stiffness can help characterize mechanical weakness or strength of each RA element, including the tunica intima, tunica media, tunica adventitia, and internal and external elastic laminae (IEL and EEL, respectively). Moreover, LM shows analog images, whereas SOS initially presents digital images, thereby rendering it easy to statistically compare the differences. Moreover, by protease incubation of the section, the vulnerability of tissue components to enzymatic digestion is comparable among different specimens.

The present study aimed to use SAM observation to clarify the association of mechanical and structural changes in RAs during aging. All sample specimens were human RAs from autopsy cases of Japanese individuals of different ages. Stiffness, blood

79 pressure, thickness of each layer, inner and outer diameters, and sensitivity to collagenase

80 digestion were compared, and aging progression was summarized in a schematic image.

Materials and methods

Subjects and ethics

The study protocol conformed to the ethical guidelines of the Declaration of Helsinki and was approved by the ethical committee of the Hamamatsu University School of Medicine (approval no. 19-180). Because the study used stored autopsy samples without a link to the patient identity, the need for written consent was waived. All procedures were conducted according to approved guidelines and regulations of the Ethic Committee.

All RAs and ascending thoracic aortae were obtained from autopsy cases of the Hamamatsu University Hospital in Japan. In total, 64 adult cadavers (48 men, 16 women) without severe cardiovascular diseases, transplantation, or hemodialysis were consecutively selected (cause of death: neoplasm in 40, inflammation in 11, circulation disorders in 4, metabolic disorders in 4, and others in 5) to investigate the effects of aging. Their ages ranged from 16 to 101 years, and the mean age was 62.9 years (standard deviation, 16.3 years). RAs at the kidney hilum were cut into round slices, and ascending aortae were dissected into longitudinal sections. When accessory or aberrant RAs were present, the main or normal RA was selected for the study. Formalin-fixed, paraffin-embedded tissue blocks were flat-sectioned into 10- μ m-thick slices and

observed with SAM. Massively calcified tissues were decalcified via soaking in a mixture of formic acid and hydrochloric acid. Sections with focal defects or uneven surfaces were omitted for measurement. Clinical data, including the cause of death and, mean blood pressure (MBP) during life, were obtained from the clinical records.

Scanning acoustic microscopic observations

We evaluated renal specimens using a SAM system (AMS-50AI; Honda Electronics, Toyohashi, Aichi, Japan) with a central frequency of 320 MHz and a lateral resolution of 3.8 μm . [10] The transducer was excited with a 2-ns electrical pulse to emit an acoustic pulse. [12] Samples were placed on the transducer, and distilled water was used for coupling fluid between the transducer and specimen. The transducer was used for both transmitting and receiving the signal. Waveforms reflected from the surface and bottom of the sample were compared to measure SOS and thickness of each point. The waveform from a glass surface without the sample served as the reference, with SOS only through water; 1495 m/s was used as a standard value.

The specimen was observed via the same method reported previously. [10] [13] Briefly, the 10- μm -thick specimen was dewaxed in xylene, washed in distilled water, and placed on the transducer. The mechanical scanner was arranged so that the

ultrasonic beam was transmitted over the specimen to provide SOS values from each point. One cross-section for each person was measured. The number of sampling points was 300 in one scanning line, and each frame comprised 300×300 points. Mean SOS values were calculated from the values of eight different areas of each layer of the RA. The points of interest were randomly selected from cross points on the lattice screen.[9] The length in SOS images, typically in an area of 1.2 or 0.6 mm², was shown on the basal horizontal or lateral left bars on the screen.

Although formalin-fixed, paraffin-embedded specimens showed slightly higher SOS than the fresh ones, SOS values were stable[14] irrespective of the length of formalin fixation (from 1 day to 3 months).[15] Therefore, sample bias resulting from the fixation condition was negligible. Areas without calcified deposits and heavy atheroma were selected for comparison because calcified areas result in chatter marks on the section, causing irregular reflection, and large atheromatous portions become translucent as a result of lipid dissolution in organic solvents.

131

132 **Light microscopic observation**

133 The same or nearby sections of SAM were stained with hematoxylin and eosin and with
134 Verhoeff's elastic and Masson's trichrome (EMT) stain for comparison. Using EMT
135 staining, the collagen and elastic fibers were stained blue and black, respectively.

136

137 **Measurement of the length of each layer and the longest** 138 **and shortest of tunica media**

139 The length of each layer was measured from LM images. The mean length was calculated
140 from at least four points of the layer. The outer and inner axes of the tunica media were
141 measured using LM images. The median length of the longest and shortest distances of
142 each axis was assessed as the lengths of the outer and inner axes, respectively.

143

144 **Catalytic damage according to collagenase digestion**

145 RAs from 3 young cadavers (40-, 44-, and 45-year-old men; "young RAs") and 3 old
146 cadavers (82- and 90-year-old men and an 81-year-old woman; "old RAs") were
147 selected for comparison. Paraffin sections were dewaxed with xylene, soaked in
148 distilled water, and submerged into a solution of phosphate-buffered saline containing

0.5 mM of calcium chloride (pH 7.4) and 250 units/mL type III collagenase (Worthington, Lakewood, NJ, USA) at 37°C for 1.5 h or for 3h.[16] The collagenase used has substrate specificity to collagens with lower proteolytic activity than other collagenases. Digested sections were first washed with distilled water before being observed with SAM. The same sections were measured 1.5 h and 3 h after digestion.

Statistical analyses

Mean SOS values were calculated from at least eight different areas per layer. The SAM manufacturer's software (LavView 2012, National Instruments, Austin, TX, USA) and commercial statistics software (Statcel3 add-in forms on Excel; OMS Publishing, Tokorozawa, Saitama, Japan), which calculated the mean areas-of-interest values, were used. Scatterplots showing the correlations between age and SOS values were established and subjected to simple linear regression analysis. The correlation strength was quantified with Pearson's correlation coefficients (r).

Mean SOS values following collagenase treatment were compared at 0, 1.5, and 3 h using paired t -test.

One-way analysis of variance was used to compare SOS values among the different age groups. Multiple comparisons were assessed using Tukey–Kramer test.

167 Before the statistical analyses were conducted, all data sets that exhibited a
168 normal distribution were compared in a test for the difference between mean values. A
169 *P* value of <0.05 was considered statistically significant for all analyses.

Results

Speed-of-sound images and their corresponding light microscopic images associated with aging

The outer shape of the young RAs was round, and with age, it gradually changed to irregular oval with dilatation (Fig 1 top). The three-layered structure comprised the tunica intima, tunica media, and tunica adventitia in young RAs, the differentiation of which progressively became obscure in middle-aged and old RAs, where IEL and EEL tended to be thinner or to disappear. Hypertrophy of the tunica intima with atherosclerosis progressed with aging.

Fig 1. Light microscopic images of the renal artery (RA) in Verhoeff's elastic and Masson's trichrome (EMT) stain and their corresponding speed-of-sound (SOS) images. Top row: EMT-stained images. Left: RA from a cadaver in its 30s. Middle: RA from a cadaver in its 50s. Right lane: RA from a cadaver in its 80s. Middle row: low-magnification SOS image. Bottom row: high-magnification SOS image. The scale bars represent 500 μm .

In SOS images (Fig 1 middle and bottom), IEL and EEL showed evidently high SOS, and the tunica media was positioned between them. These laminae were thick and continuous in young RAs and tended to be thinner and interrupted in old RAs. The tunica

media was composed of thick, condensed smooth muscles with high SOS in young RAs and gradually changed to lean, sparse smooth muscles with low SOS in old RAs. Tunica intima accumulated atheromatous lipid material with low SOS values. Tunica adventitia, mainly composed of collagen bundles, displayed no remarkable changes in SOS with aging.

Fig 2a is a scatterplot of age and mean SOS values of the middle RA layer. The individual dot represents the mean SOS of each person. Linear regression fit showed a significant inverse correlation between age and SOS of the tunica media ($n = 64$, $r = -0.37$, $P = 0.0027$).

Fig 2. Relationship between age and speed-of-sound (SOS) values. (a) Scatterplot of age and average SOS values of the tunica media of the renal artery (RA). The individual dot represents the average SOS of each person. Linear regression fit showed a statistically significant inverse correlation between age and SOS of RA ($n = 64$, $r = -0.37$, $P = 0.0027$). (b) Speed-of-sound values of internal (IEL) and external (EEL) elastic laminae associated with aging. Both SOS values demonstrated reverse correlations with age ($n=36$, for IEL, $r = -0.369$, $P = 0.0026$; for EEL, $r = -0.643$, $P = 0.000000183$).

Speed-of-sound values of internal and external elastic laminae

associated with aging

SOS of IEL and EEL significantly decreased with aging (Fig 2b). Both SOS values presented reverse correlation with age ($n=36$, IEL: $r = -0.369$, $P = 0.0026$; EEL: $r = -0.643$, $P = 0.000000183$).

Relationship between speed-of-sound values of tunica media and mean blood pressure

Fig 3a shows the inverse correlation between MBP and SOS values of the tunica media ($n = 37$, $r = -0.37$, $P = 0.0019$). In RAs from cadavers who had had higher BP, SOS values in the tunica media were lower. Systolic and diastolic pressures and PP significantly increased with age (Fig 3b; for systolic pressure, $n=37$, $r = 0.44$, $P = 0.00018$; for diastolic pressure, $n=37$, $r = 0.36$, $P = 0.0024$; and for PP, $r = 0.32$, $P = 0.0076$).

Fig 3. Relationship between age and blood pressure. (a) Inverse correlation between mean blood pressure (MBP) and speed-of-sound (SOS) values of tunica media. In renal arteries (RAs) with higher blood pressure, SOS values in the tunica media were lower. (b) Systolic and diastolic blood pressure associated with aging. Systolic and diastolic pressor pressures increased significantly with age (for systolic pressure, $r = 0.44$, $P =$

0.00018; for diastolic pressure, $r = 0.36$, $P = 0.0024$). The pulse pressure also increased significantly with aging ($r = 0.32$, $P = 0.0076$).

Thickness of the three layers associated with aging

Fig 4a depicts the alteration in the width of each segment of RAs with aging. The widths of the tunica media and tunica adventitia showed no remarkable changes, whereas tunica intima exhibited remarkably increased thickness with aging ($n=35$, $r = 0.43$, $P = 0.0002$).

Fig 4. Thickness of each layer of the renal artery (RA) with aging. (a) The width of the three layers with aging. The thickness of the tunica media and tunica adventitia showed no remarkable changes, whereas the tunica intima exhibited increased thickness with aging ($n=35$, $r = 0.43$, $P = 0.0002$). (b) The outer and inner axes of tunica media with aging. Both the outer and inner axes of the tunica media significantly increased with aging. As a consequence, the renal artery (RA) became dilated with aging.

Thickness of the outer and inner mean axes of the tunica media

Although the width of the tunica media was rather stable with aging, the outer and inner mean axes of the tunica media gradually expanded with age (Fig 4b; for the outer axis,

n=35, $r = 0.332$, $P = 0.0068$; for the inner axis, n=35, $r = 0.511$, $P = 0.000133$). As a consequence, RAs became dilated with aging.

Comparison between speed-of-sound values of renal artery and aorta

The alteration in SOS values in the tunica media of RAs was compared with that of the ascending aorta (Fig 5a). Both SOS values progressively increased with aging. SOS of the RA was always lower than that of the aorta, and the correlation was positive (Fig 5b; n=33, $r = 0.51$, $P = 0.000146$).

Fig 5. Relationship of speed-of-sound (SOS) values of the renal artery (RA) and ascending aorta with aging. (a) SOS values of tunica media of RAs and ascending aorta with aging. Both SOS values progressively decreased with aging. SOS values of the aorta decreased following those of RAs (n=33, $r = -0.35$, $P = 0.0043$). (b) Relationship between speed-of-sound (SOS) values of the renal artery (RA) and the aorta. SOS of the ascending aorta was positively correlated with that of the RA (n=33, $r = 0.51$, $P = 0.0000146$).

Difference in sensitivity to collagenase treatment between

young and old renal arteries

Owing to collagenase treatment, SOS values in the tunica media progressively decreased in young RAs, whereas they remained stable in old RAs (Fig 6). Young tunica media with rich smooth muscles and elastic fibers showed reduced SOS values. In contrast, old tunica media with abundant collagen fibers and reduced smooth muscles maintained stable SOS values during digestion, particularly the inner side near intima. Statistical analysis showed a significant decline in SOS values in young RAs compared with old RAs (Fig 7).

Fig 6. Difference in sensitivity to collagenase digestion between young and old renal arteries (RAs). Speed-of-sound (SOS) values before digestion were higher in the tunica media of young renal arteries (RAs) than in old RAs, and they reduced rapidly after digestion. However, old RAs were rather resistant to enzymatic degradation. The corresponding LM images in Verhoeff's elastic and Masson's trichrome stain were shown on the SAM images (left; before digestion, right; 3 h after digestion). The scale bars represent 500 μ m.

Fig 7. Difference of susceptibility to collagenase digestion associated with aging. Speed-of-sound (SOS) values before digestion were higher in the tunica media of young renal arteries (RAs) than in that of old RAs, and they reduced rapidly after digestion. However, old RAs were rather resistant to enzymatic degradation. The graph shows a

significant decline in SOS of young RAs in comparison with old RAs. $**P<0.01$, $*P<0.05$

Summary of RA alteration in structure and fragility associated with aging

Fig 8 shows the schematic image changes in RAs associated with aging. Young RAs had round, regular three-layered structure with continuous, thick EEL and IEL. Old RAs had an irregular oval structure with hypertrophy of the tunica intima due to atherosclerosis. Tunica media of old RAs exhibited a decrease in smooth muscles and had elastic fiber splitting. In terms of mechanical strength, young RAs showed high SOS values in the tunica media, EEL, and IEL, indicating the high stiffness of these structures. In contrast, old RAs revealed irregularly low SOS values in the tunica media, EEL, and IEL, indicating the loss of mechanical strength in these structures.

Fig 8. Schematic image alterations of renal arteries (RAs) associated with aging. The outer shape of the RAs changes from round to oval with inward and outward hypertrophy. The tunica intima stiffens with atherosclerosis, and the tunica media expands with a reduction in smooth muscle and splitting of elastic fibers.

Discussion

Virtual histological images constructed from SOS values corresponded well with LM images and demonstrated alterations associated with aging. Older RAs became elliptical with hypertrophy of the tunica intima due to atherosclerosis. SOS of the tunica media progressively decreased with aging, which indicated mechanical weakness and was correlated with muscular atrophy and disappearance. Moreover, SOS values of EEL and IEL reduced with aging, indicating a loss of elasticity in old RAs. These results suggest that RAs stiffen with age mainly because of intimal atherosclerosis and accompanied degeneration of other layers with loss of muscle and elastic fibers. The hypertrophy of the tunica intima may compensate for the mechanical weakness of the outer layer to bear high BP.

Although arteries stiffen with age, the present study showed that SOS values lowered in proportion with age and BP. PWV and PP are the two significant indices of arterial stiffness[3] that typically increase with age.[4][17] PWV is assessed by measuring transit distance and transit time between two sites in arteries, such as carotid and femoral arteries. Pressure waveforms are simultaneously recorded by placing BP cuffs around the neck and upper thigh. Arterial distensibility, a measure of the artery's ability to expand and contract with cardiac pulsation and relaxation, correlates with the

degree of atherosclerosis, i.e., the intimal stiffness.[18][19] The present study reflected no intimal stiffness because tissue preparation procedures led to the loss of original intimal properties such as lipid accumulation and calcification. The discrepancy of the results depends on the areas assessed. PWV and SOS mainly calculate intimal and medial stiffness, respectively.

Some studies have already reported the relationship between SOS values and BP. Akhtar *et al.* stated that SOS had an inverse relationship with systolic and diastolic blood pressure in aortic biopsies.[20] Diabetic aorta—one of the causes of hypertension—showed reduced SOS in vessel walls, particularly in the interlamellar regions of the tunica media in an experimental rat model.[21] These regions corresponded to the extracellular matrix in which protease activity was increased in diabetic vessels. Fibrillin microfibrils, one of the extracellular matrix proteins, were significantly shorter in diabetic rats than in healthy controls. Reduced muscle fibers and microfibril fragmentation may cause mechanical weakness of the tunica media. Atherosclerotic intimal lesions reportedly cause increased SOS values.[22]

Old RAs showed resistance to protease digestion in comparison with young RAs. Young RAs with concentrated muscles and regular elastic fibers showed more vulnerability to collagenase, as observed in thoracic aortae.[13] Old RAs with split elastic

fibers and reduced smooth muscles, which had been replaced by collagen fibers, were already affected or modified to become resistant to protease digestion. Therefore, the extracellular matrix components of old RAs were maintained after digestion.

With aging, the tunica media lost its stiffness and its diameter enlarged; however, its thickness remained stable, which may be an adaptive response to high BP. This outward hypertrophic remodeling corresponds to that in animal models of normal aging.[17] Collagen fibers (via fibrosis) and extracellular matrix components fill the space among smooth muscles in old RAs. Computed tomographic angiography in adults revealed that mean RA diameter increased from the 10s to 50s, was rather stable up to 70s, and rapidly decreased after 80s in the Nigerian population.[23] This result showed that adult RAs usually become dilated with aging and finally reveal luminal stenosis via atherosclerosis, consistent with the present autopsy cases. The present research involved autopsy cases in which the patients had had chronic debilitating diseases. Therefore, degenerative changes in the tunica media of these cases were more severe than those observed in the tunica media of healthy adults.

SOS values in the ascending aorta were positively correlated with those in the RA (Fig 5b). Both vessels have a similar structure consisting of smooth muscles and elastic fibers.[1] Aortic pulse waves are conducted to RAs; therefore, RA pressure is

always lower than the aortic pressure. It is reasonable that SOS values of RA are lower than those of aorta in all ages (Fig 5a).

In my previous study, SOS values in the thoracic aorta were negatively correlated with age.[13] Older aortae showed more significant degeneration of the tunica media with low SOS values. These aortae expressed specific extracellular matrix components to compensate for mechanical weakness. RAs with a similar decrease in SOS values associated with aging exhibited similar histology, probably following the same process. The resistance of old RAs to collagenase digestion signified that older RAs possessed more modification or bridging of proteins.[15][24]

This study had several limitations. First, all samples were obtained from autopsy cases, of which a high percentage represented patients with neoplasms. Most patients with tumors had received numerous types of therapies that nutrition was in a poor state. This state of malnutrition might cause reduced lipid accumulation in the tunica intima. Prolonged formalin fixation might influence SOS measurement; however, Sasaki et al.[14] reported that the influence of formalin fixation on the acoustic properties of the healthy kidney was minimal. No significant change in acoustic parameters, including SOS, was found. Second, location bias might influence the results. RAs with severe focal calcification could not be cut into flat sections; therefore, these hard portions were

excluded from the study. Decalcification procedure by soaking in acid solution may influence SOS values. Third, the height and weight of the cadavers were not considered; therefore, the influence of body size on the findings was not assessed. Although the RA size was correlated with body size, renal function remained in the normal range and might have changed during aging; owing to this reason, raw data were used.

Conclusions

This study revealed the utility of SAM observation, which simultaneously showed structural and mechanical information from a histological glass slide. It provided objective evidence of damage or degeneration in each portion of the RA. The fact that arteries become stiffer with aging originates from intimal atherosclerosis and not from medial degenerative changes. SAM investigation disclosed the association between aging-related structural and functional alterations.

Acknowledgments

The author thanks T. Moriki, Y. Egawa, Y. Kawabata, and N. Suzuki for their assistance in the preparation of the histological samples, Dr. K. Kobayashi (Honda Electronics) for his technical support and advice with SAM, and Enago (www.enago.jp)

384 for the English language review.

385

References

1. Lacolley P, Regnault V, Segers P, Laurent S. Vascular smooth muscle cells and arterial stiffening: Relevance in development, aging, and disease. *Physiol Rev.* 2017;97(4):1555–617. doi:10.1152/physrev.00003.2017.
2. Jia G, Aroor AR, Sowers JR. Arterial stiffness : a nexus between cardiac and renal disease. *Cardiorenal Med.* 2014;4:60–71. doi:10.1159/000360867
3. Safar ME, Plante GE, Mimran A. Arterial stiffness, pulse pressure, and the kidney. *Am J Hypertens.* 2015;28(5):561–9. doi:10.1093/ajh/hpu206
4. Mitchell GF, Parise H, Benjamin EJ, Larson MG, Keyes MJ, Vita JA, et al. Changes in arterial stiffness and wave reflection with advancing age in healthy men and women, the Framingham heart study. 2004; doi:10.1161/01.HYP.0000128420.01881.aa
5. Miyawaki NB, Lester PE. Chapter 13 : Vascular Disease in the Elderly. In: Geriatric nephrology curriculum. 2009. p. 1–5.
6. Antonio F, Borelli DO, Pinto IMF, Amodeo C, Paola EP, Kambara AM, et al. Analysis of the sensitivity and specificity of noninvasive imaging tests for the diagnosis of renal artery stenosis. 2013;423–33. doi:10.5935/abc.20130191

- 404 7. Denic A, Glassock RJ, Rule AD. Structural and functional changes with the
405 aging kidney. *Adv Chronic Kidney Dis.* 2016;23(1):19–28.
406 doi:10.1053/j.ackd.2015.08.004
- 407 8. Saijo Y. Acoustic microscopy: latest developments and applications. *Imaging*
408 *Med [Internet].* 2009;1(1):47–63. doi:10.2217/iim.09.8.
- 409 9. Miura K, Yamamoto S. Pulmonary imaging with a scanning acoustic microscope
410 discriminates speed-of-sound and shows structural characteristics of disease. *Lab*
411 *Investig.* 2012; 92:1760-65. doi:10.1038/labinvest.2012.135
- 412 10. Miura K, Yamamoto S. Histological imaging from speed-of-sound through
413 tissues by scanning acoustic microscopy (SAM). *Protoc Exch.* 2013;
414 doi:10.1038/protex.2013.040
- 415 11. Miura K, Mineta H. Histological evaluation of thyroid lesions using a scanning
416 acoustic microscope. *Pathol Lab Med Int.* 2014; doi:10.2147/plmi.s58343
- 417 12. Hozumi N, Yamashita R, Lee CK, Nagao M, Kobayashi K, Saijo Y, et al. Time-
418 frequency analysis for pulse driven ultrasonic microscopy for biological tissue
419 characterization. In: *Ultrasonics.* 2004. p. 717–22.
420 doi:10.1016/j.ultras.2003.11.005
- 421 13. Miura K, Yamashita K. Mechanical weakness of thoracic aorta related to aging or

- 422 dissection predicted by speed of sound with collagenase. *Ultrasound Med Biol.*
- 423 2019;45(12):3102–15. doi:10.1016/j.ultrasmedbio.2019.08.012
- 424 14. Sasaki H, Saijo Y, Tanaka M, Okawai H, Terasawa Y, Yambe T, et al. Influence
- 425 of tissue preparation on the high-frequency acoustic properties of normal kidney
- 426 tissue. *Ultrasound Med Biol.* 1996;22(9):1261–5. doi:10.1016/S0301-
- 427 5629(96)00150-0.
- 428 15. Miura K, Egawa Y, Moriki T, Mineta H, Harada H, Baba S, et al. Microscopic
- 429 observation of chemical modification in sections using scanning acoustic
- 430 microscopy. *Pathol Int.* 2015;65(7):355–66. doi:10.1111/pin.12288
- 431 16. Miura K, Katoh H. Structural and histochemical alterations in the aortic valves of
- 432 elderly patients: a comparative study of aortic stenosis, aortic regurgitation, and
- 433 normal valves. *Biomed Res Int.* 2016; 6125204. doi:10.1155/2016/6125204
- 434 17. Nyhan D, Steppan J, Barodka V, Berkowitz DE. Vascular stiffness and increased
- 435 pulse pressure in the aging cardiovascular system. *Cardiol Res Pract.* 2011;1(1).
- 436 doi:10.4061/2011/263585
- 437 18. Lee HY, Oh BH. Aging and arterial stiffness. *Circ J.* 2010;74(11):2257–62.
- 438 doi:10.1253/circj.CJ-10-0910.
- 439 19. O’Rourke MF, Staessen JA, Vlachopoulos C, Duprez D, Plante GE. Clinical

- applications of arterial stiffness; definitions and reference values. *Am J Hypertens.* 2002;15(5):426–44. doi:10.1016/S0895-7061(01)02319-6
20. Akhtar R, Cruickshank JK, Zhao X, Derby B, Weber T. A pilot study of scanning acoustic microscopy as a tool for measuring arterial stiffness in aortic biopsies. *Artery Res.* 2016;13:1–5. doi:10.1016/j.artres.2015.11.001
21. Akhtar R, Cruickshank JK, Zhao X, Walton LA, Gardiner NJ, Barrett SD, et al. Localized micro- and nano-scale remodelling in the diabetic aorta. *Acta Biomater.* 2014;10(11):4843–51. doi:10.1016/j.actbio.2014.07.001
22. Saijo Y, Ohashi T, Sasaki H, Sato M, Jorgensen C, Nitta S. Application of scanning acoustic microscopy for assessing stress distribution in atherosclerotic plaque. *Ann Biomed Eng.* 2001;29:1048–53. doi:10.1114/1.1424912
23. Chiaganam NO, Ekpo EU, Egbe NO, Nzotta CC, Okwara KK. Aging and the average diameter of the renal artery using computed tomography angiography (CTA). *South African Radiogr.* 2013;51(1):23–5.
24. Santos AL, Lindner AB. Protein posttranslational modifications : roles in aging and age-related disease. 2017;2017: 5716409. doi:10.1155/2017/5716409

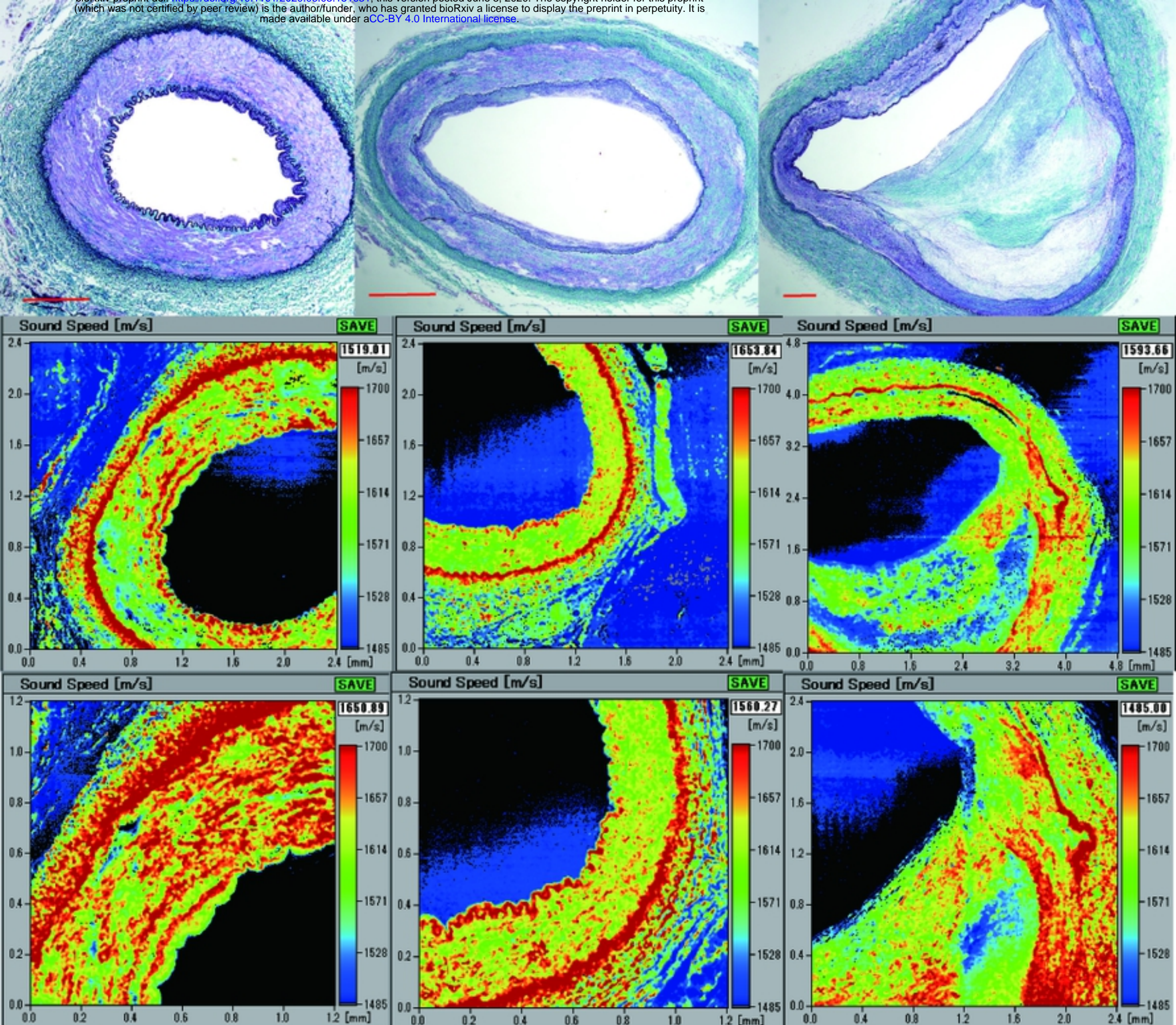


Figure 1

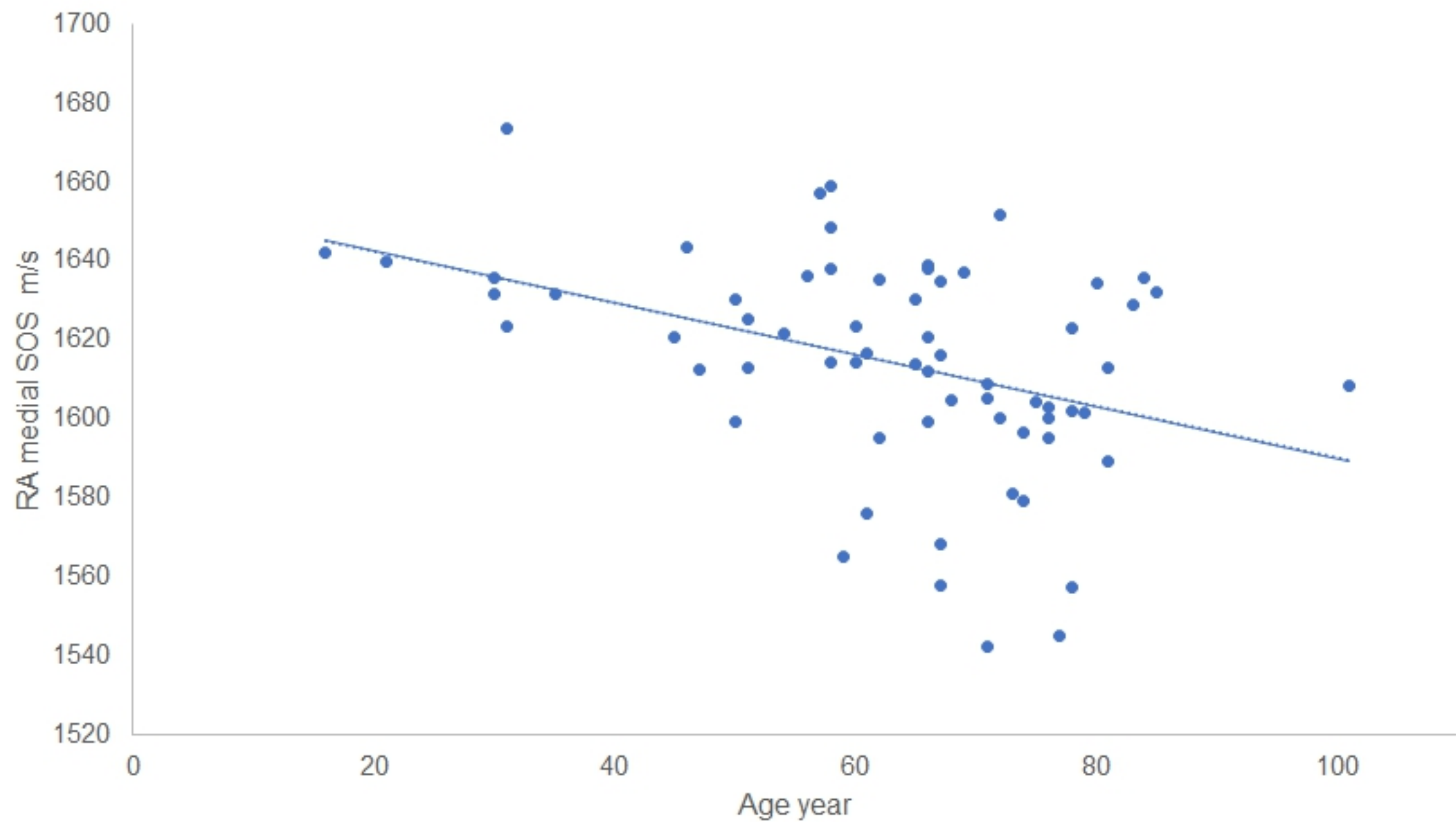


Figure 2a

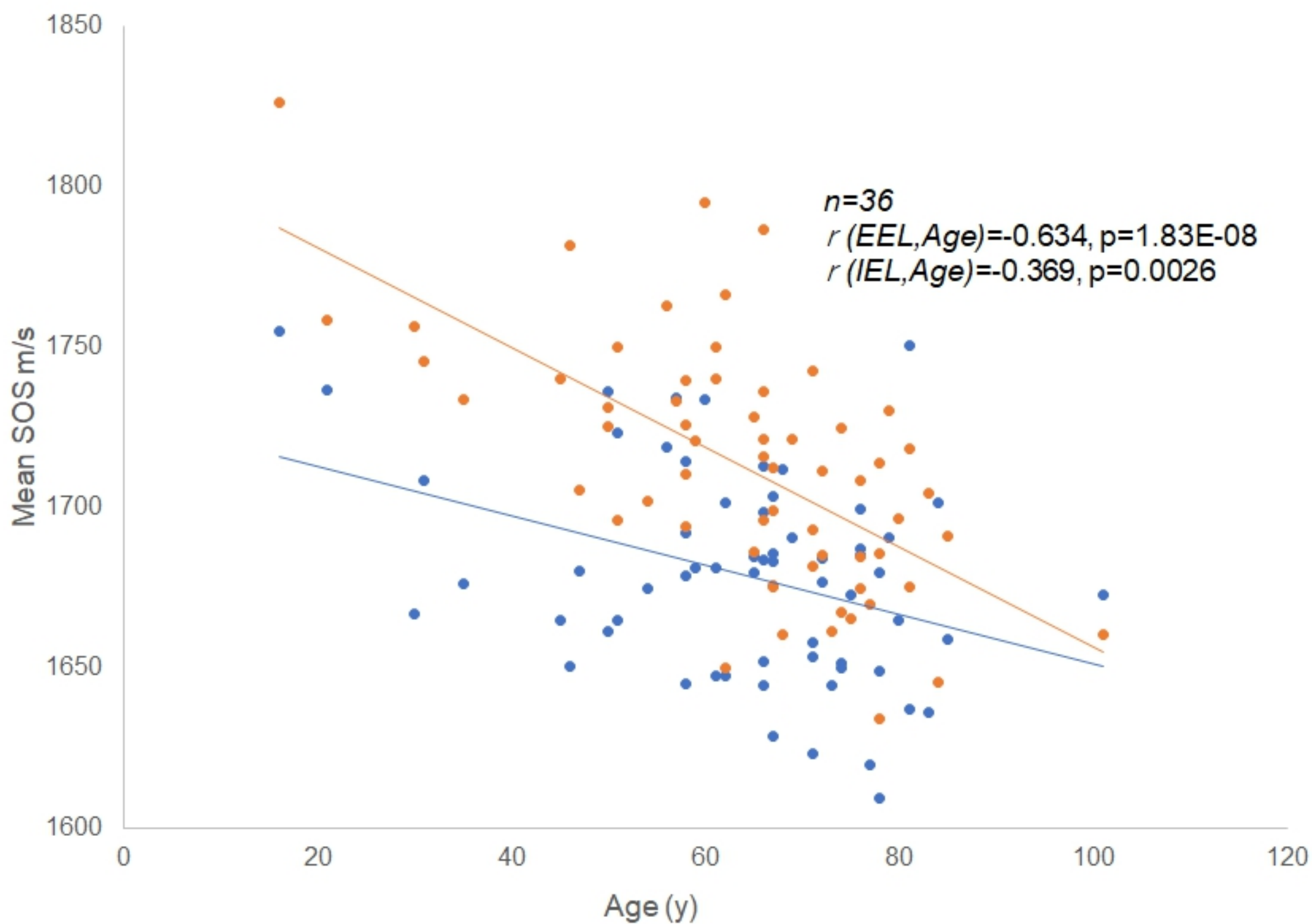


Figure 2b

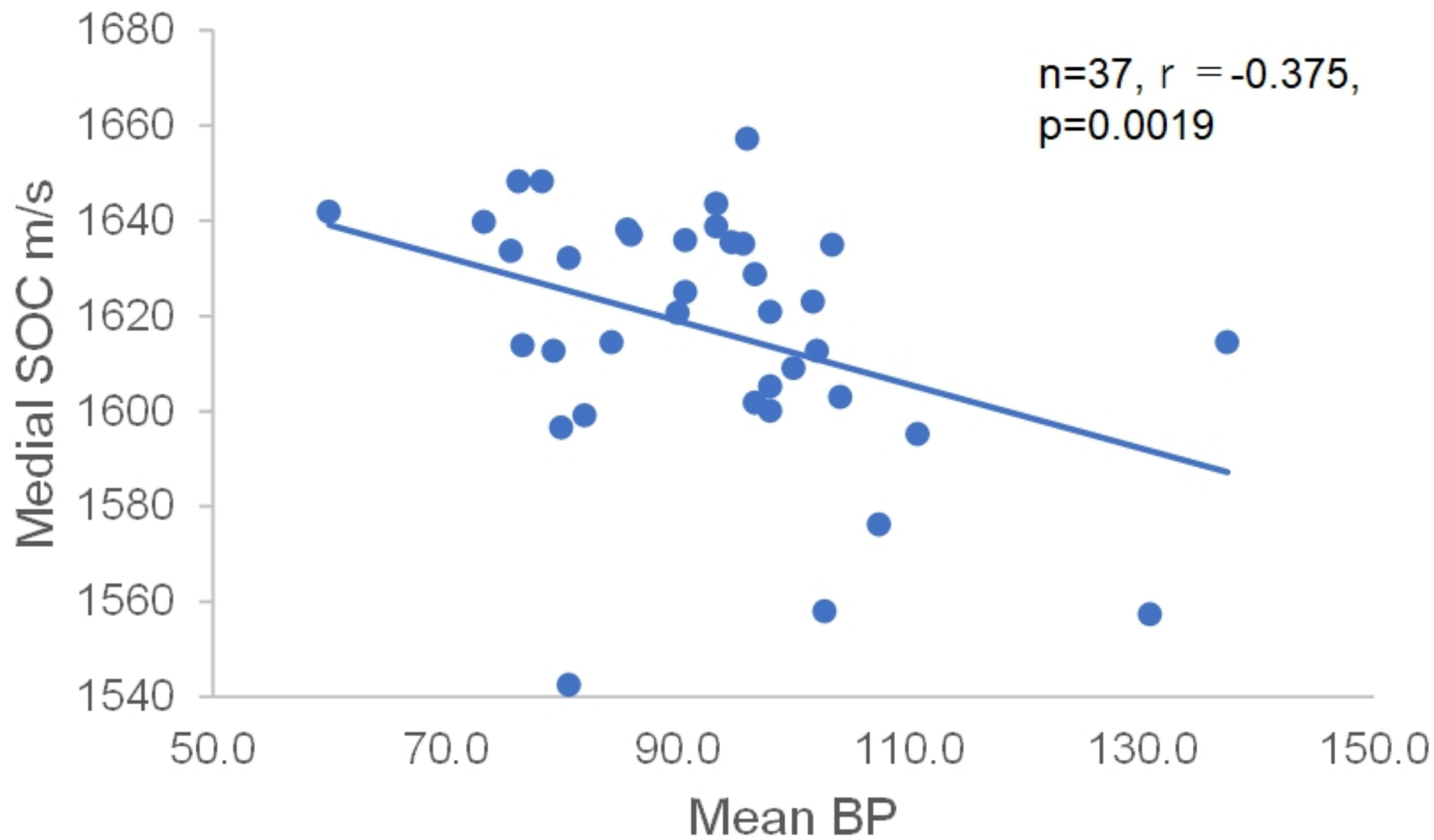


Figure 3a

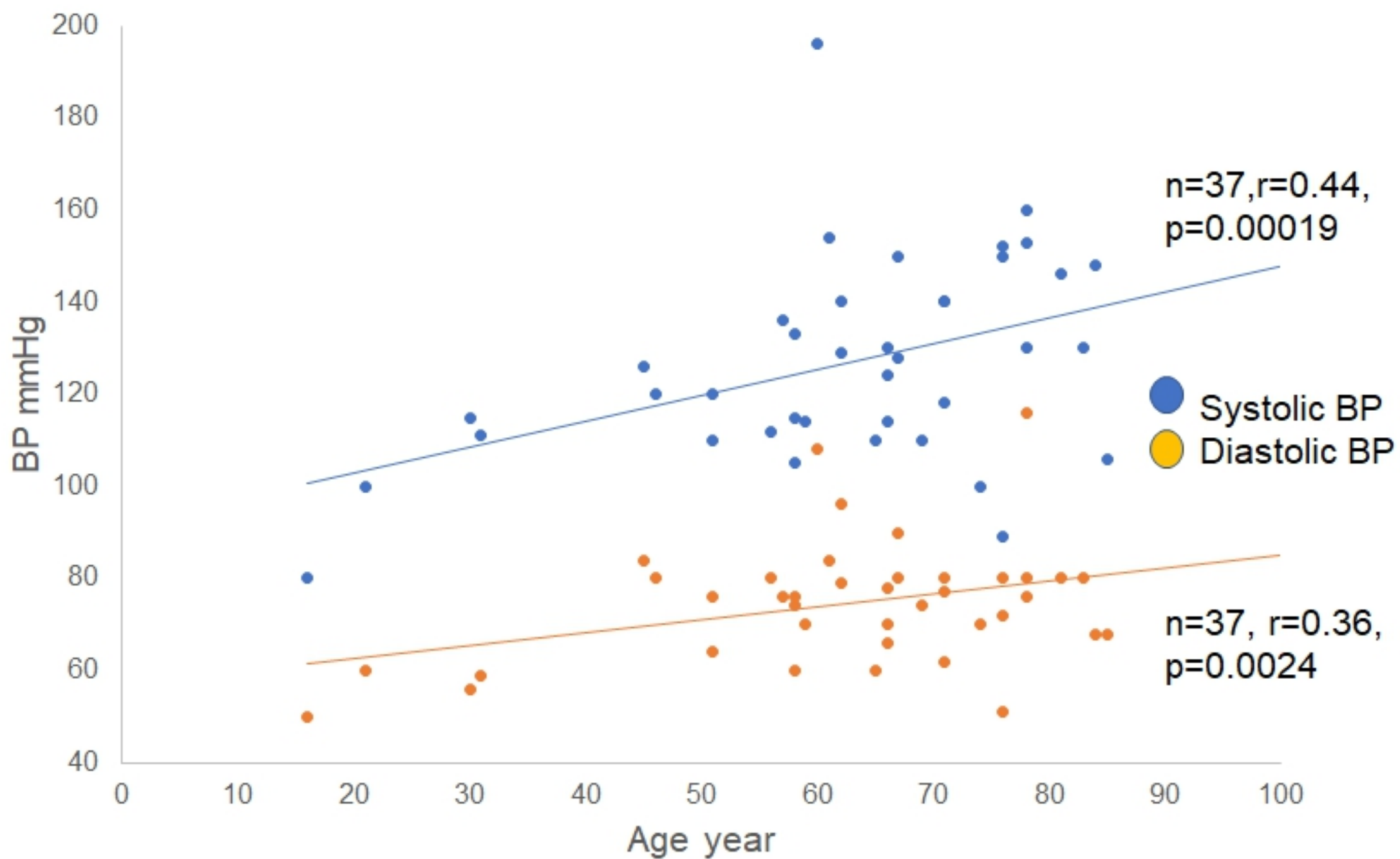


Figure 3b

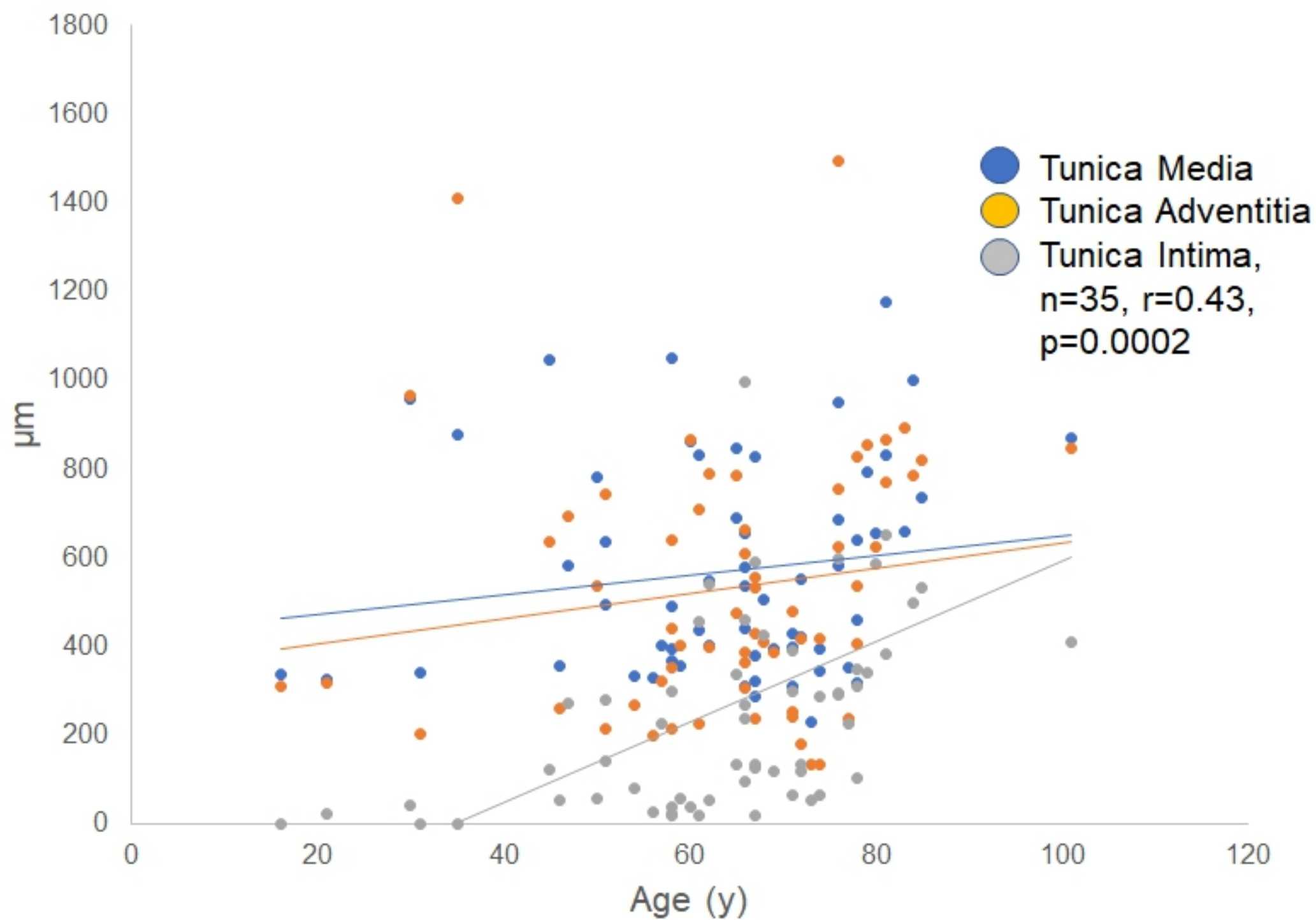


Figure 4a

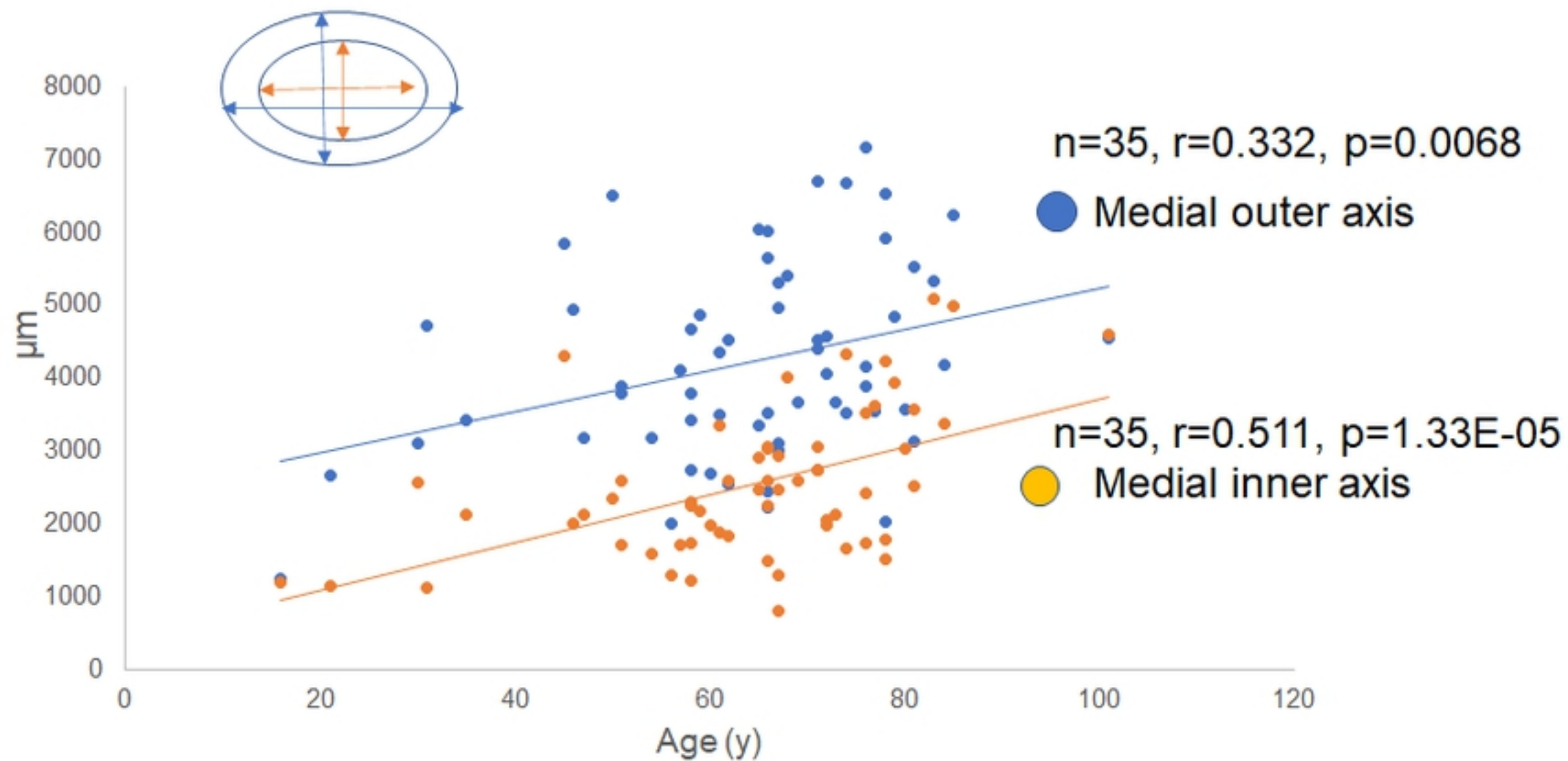


Figure 4b

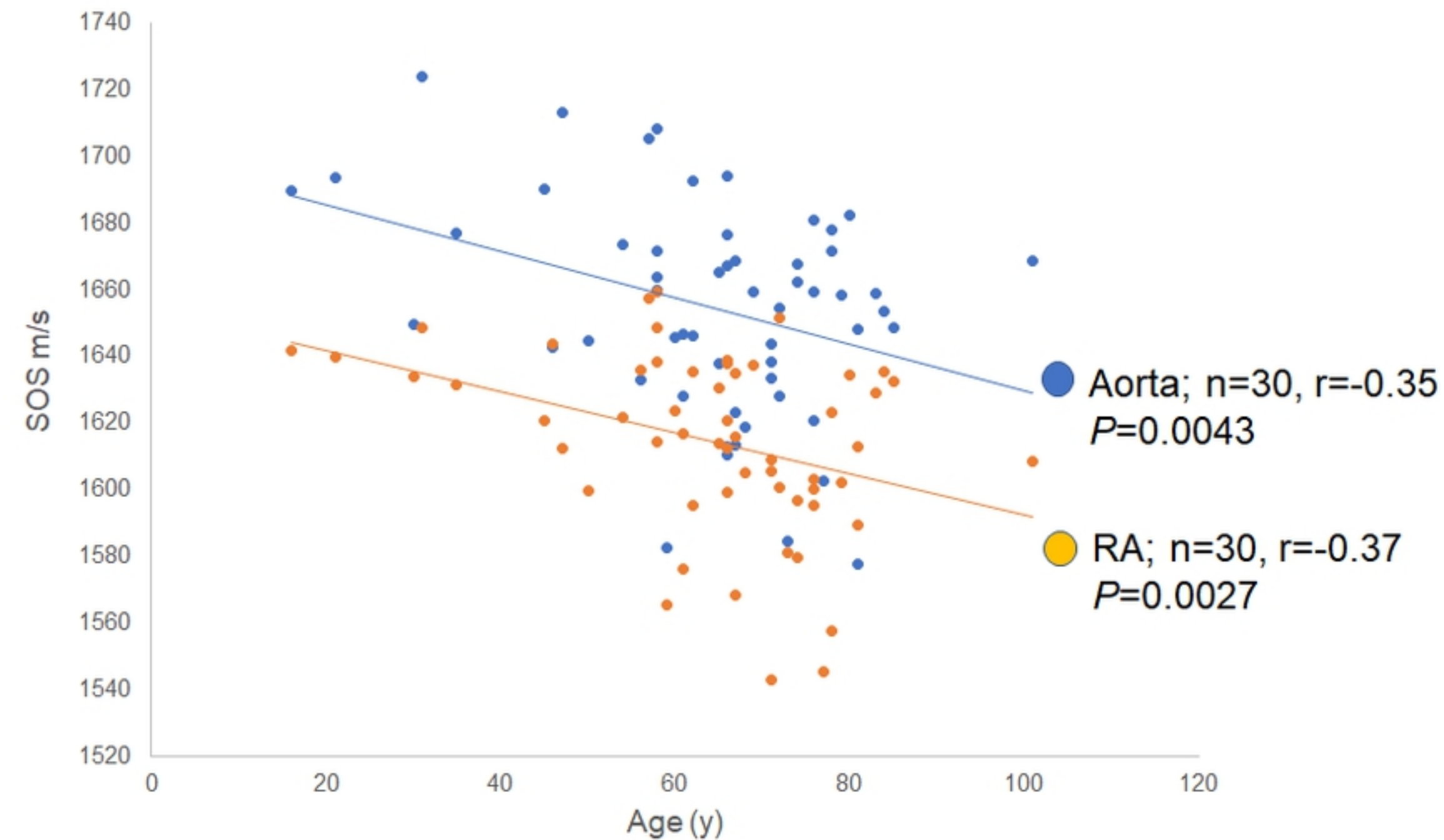


Figure 5a

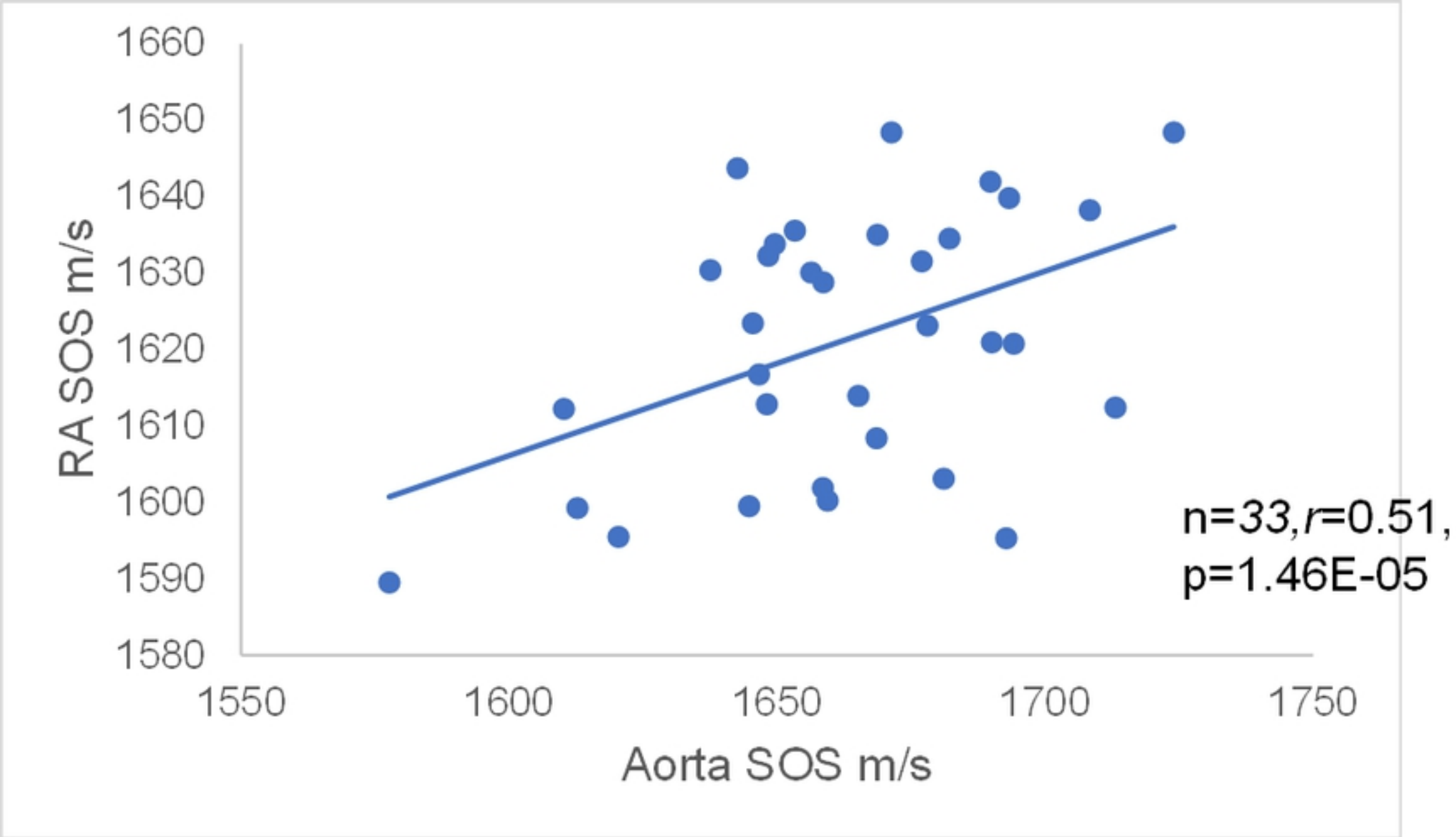
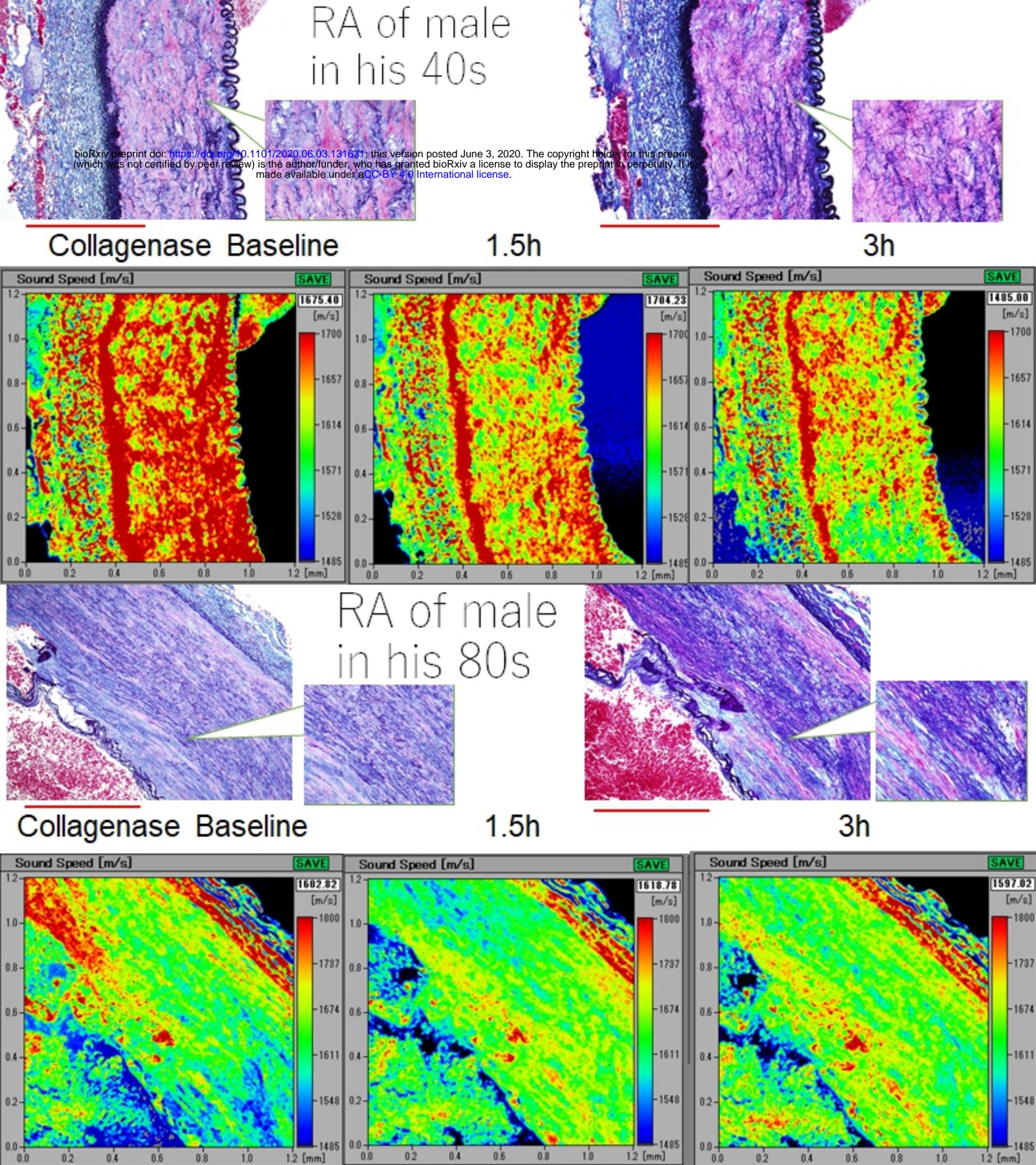


Figure 5b



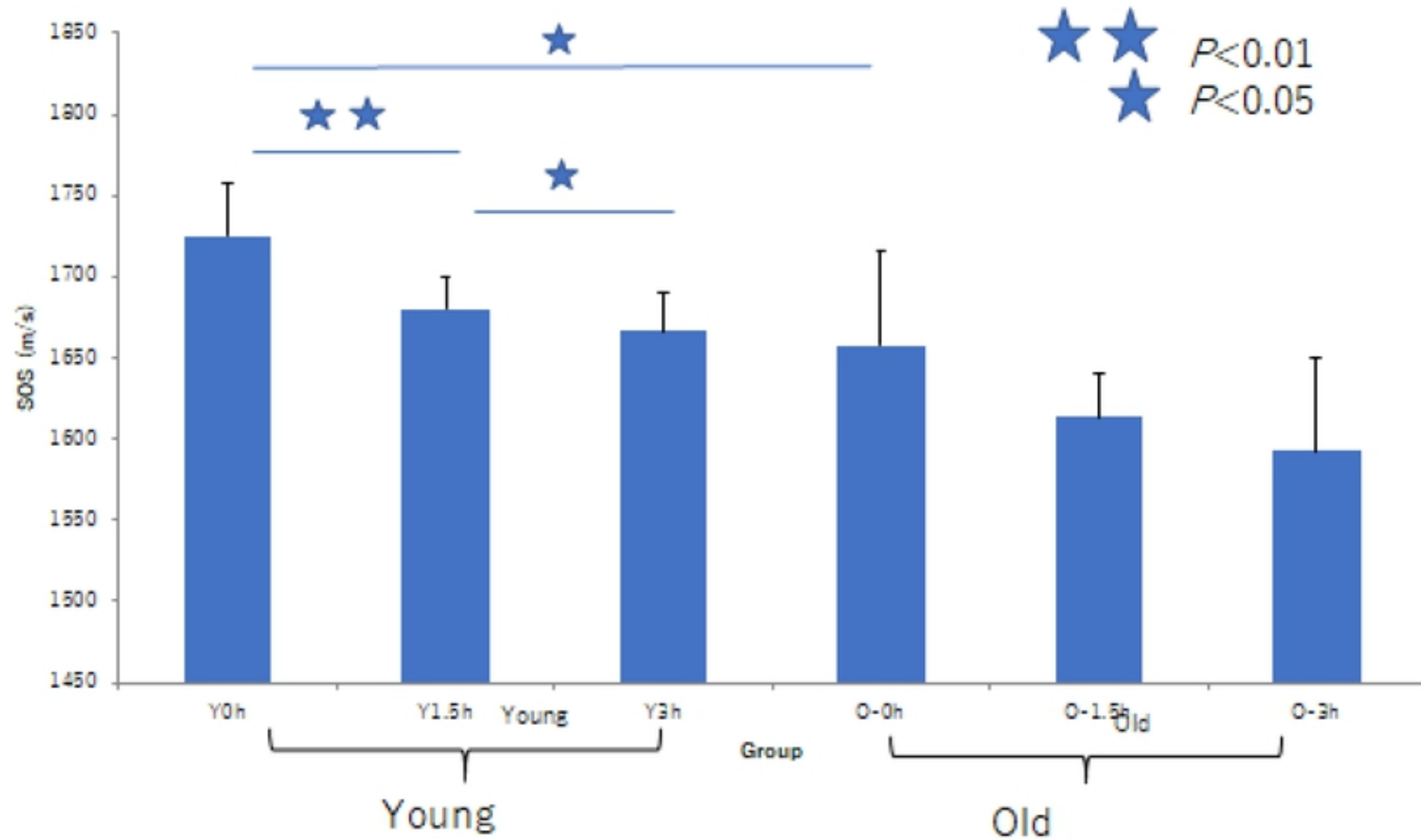


Figure 7

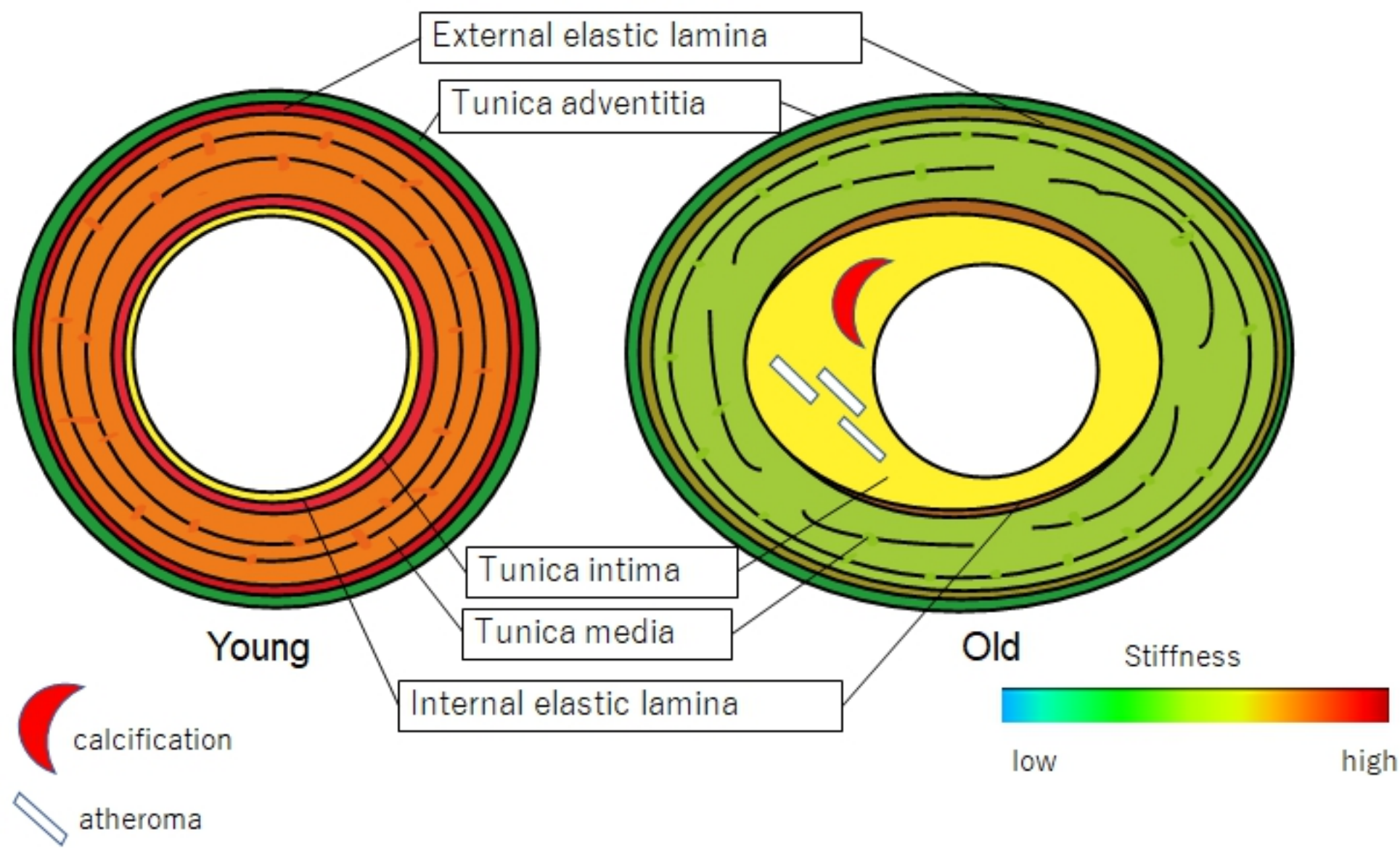


Figure 8